Supplementary Information for

Nitrogen-Coordinated Single-Atom Catalysts with Manganese and Cobalt Sites for Acidic Oxygen Reduction

Guojie Chao[1], Yizhe Zhang[1], Longsheng Zhang[1*], Wei Zong[2], Nan Zhang[1], Tiantian Xue[2], Wei Fan[2], Tianxi Liu[1], Yi Xie[3*]

[1]Key Laboratory of Synthetic and Biological Colloids, Ministry of Education, School of Chemical and Material Engineering, International Joint Research Laboratory for Nano Energy Composites, Jiangnan University, Wuxi, China
[2]State Key Laboratory for Modification of Chemical Fibers and Polymer Materials College of Materials Science and Engineering, Donghua University, Shanghai, China
[3]Hefei National Laboratory for Physical Sciences at Microscale, University of Science and Technology of China, Hefei, China

**Correspondence and requests for materials should be addressed to Longsheng Zhang (zhangls@jiangnan.edu.cn), Yi Xie (yxie@ustc.edu.cn).*

This file includes:

Materials and Methods.

Fig. S1 to S15.

Table S1 to S2.

Materials and Methods

Chemicals

Zinc nitrate hexahydrate, manganese acetate tetrahydrate, cobalt acetate tetrahydrate and methanol were brought from Sinopharm Chemical Reagents. 2-methylimidazole, Nafion, hexane and methyl alcohol were brought from Sigma-Aldrich. Commercial Pt/C (20 wt%) catalyst was brought from Alfa Aesar. All chemicals were used without further purification.

Synthesis of catalysts

As shown in Fig. S1, the MnCo-N-C catalyst was synthesized based on zeolitic imidazolate framework-8 (ZIF-8). Firstly, the manganese-doped ZIF-8 precursor (denoted as Mn-ZIF) was synthesized *via* a solvent method. In a typical procedure, zinc nitrate hexahydrate (4 mmol) and manganese acetate tetrahydrate (1 mmol) were dissolved in 40 mL of methanol under stirring, followed by addition of 40 mL methanol of 2-methylimidazole (16 mmol). The solution was aged for 24 h and the precipitates would appear. Then the precipitate was centrifuged and washed with methanol three times and dried in vacuum at 60 ℃ for overnight to obtain Mn-ZIF powder. Afterwards, the Mn-ZIF (50 mg) was dispersed in 10 mL of hexane by sonication for 1 h at room temperature. Then, 200 μL of cobalt acetate tetrahydrate solution (18.5 mg mL^{-1}) was added to the above solution drop by drop under stirring. The mixed solution was treated with ultrasound at room temperature for 2 h. The precipitate was collected and dried in vacuum at 60 ℃ for overnight to obtain Co doped Mn-ZIF precursor (denoted as Mn/Co-ZIF). Finally, the Mn/Co-ZIF precursor was placed in a tube furnace and carbonized at 950 ℃ for 2 h with a heating rate of 2 ℃ min^{-1} under flowing argon gas to obtain catalysts of Mn-, Co- and N-doped carbon (MnCo-N-C). Accordingly, the Co-N-C catalyst was synthesized *via* a similar procedure without manganese acetate tetrahydrate.

Characterization

The morphologies of samples were observed by using scanning electron microscopy

(JSM-7500F, JEOL), transmission electron microscopy (JEM-2100F, JEOL) and high angle annular dark-field scanning transmission electron microscopy (HAADF-STEM) with a Tecnai G2 20 TWIN TEM under an acceleration voltage of 200 kV. X-ray diffraction patterns were obtained from the X' Pert Pro X-ray diffractometer with Cu Kα radiation (λ = 0.1542 nm). Raman scattering spectrum was recorded with a Renishaw in Via Raman Spectrometer using the laser wave length of 633 nm. The Co *K*-edge X-ray absorption spectroscopy data of samples and references were collected on 1W1B beamline at Beijing Synchrotron Radiation Facility. The X-ray photoelectron spectroscopy (XPS) spectra were obtained from a VG ESCALAB 220I-XL device. Inductively coupled plasma-mass spectrometry (ICP-MS, iCAP7400, Thermo-Fisher) were employed to quantify the content of metal elements in the samples.

The attenuated total reflectance surface enhanced infrared absorption spectroscopy (ATR-SEIRAS) experiments were taken with Nicolet 6700 FTIR spectrometer with an electrochemical Cell (Linglu instruments, Shanghai) on a PIKE VeeMAX III variable angle ATR sampling accessory. The spectral resolution was set to 8 cm^{-1}. The spectra are given in absorption units defined as $A = -\log(R/R_0)$, where R and R_0 represent the reflected infrared intensities corresponding to the sample and reference-single beam spectrum, respectively. A 60° Si face-angled crystal was used as reflection crystal. The thin Au film was deposited chemically on Si crystal for signal enhancement. The electrocatalyst was dropped onto Au film to serve as a working electrode for SEIRAS experiments with the loading of 0.08 mg cm^{-2}. Platinum wire and Ag/AgCl electrode were employed as counter and reference electrode, respectively. The O_2-saturated 0.5 M H_2SO_4 aqueous solution was used as the electrolyte. Chronopotentiometry method was used at different potentials (0.9 to 0.1 V *vs.* Ag/AgCl). The SEIRAS spectra were collected during the chronopotentiometry test.

Electrochemical Measurements

Electrochemical measurements were conducted using graphite rod and Ag/AgCl as the counter and reference electrode, respectively. Typically, the as-prepared catalysts (5 mg) were added into a mixed solution of ethanol (0.35 mL) and Nafion solution (0.095 mL). The solution was subjected to ultrasonication for 30 min to prepare a homogeneous ink. Then, working electrode was prepared by depositing 5 μL of the catalyst ink onto rotating disk electrode (5 mm in diameter). Cyclic voltammetry (CV) was measured in N_2 or O_2-saturated 0.5 M H_2SO_4 aqueous electrolytes at 50 mV s^{-1}. Linear sweep voltammetry (LSV) was measured onto rotating disk electrode with a rotation speed of 1600 rpm at 10 mV s^{-1}. The current-time (*i*-t) chronoamperometric measurement was conducted at a constant potential of 0.7 V (*vs.* reversible hydrogen electrode, RHE) with a rotation speed of 200 rpm. Accelerated durability test of 5000 cycles was conducted by using CV from 0.6 to 1.0 V (*vs.* RHE) at a rotation speed of 1600 rpm with a scan rate of 100 mV s^{-1} for 5000 cycles. Methanol toxicity evaluation of catalyst was performed using the *i*-t response at 0.7 V (*vs.* RHE) at a rotation speed of 1600 rpm in O_2-saturated electrolytes with or without 1 M of methyl alcohol.

For the rotating ring disk electrode (RRDE) test, the working electrode was prepared by depositing 7.5 μL of the catalyst ink onto the glassy carbon disk electrode (6.25 mm in diameter). The ring electrode potential was set at 1.2 V (vs. RHE), and the LSV curve was recorded with a scan rate of 10 mV s^{-1} at 1600 rpm. The electron transfer number (n) and hydrogen peroxide yield (y) were calculated by the following equations:

$$n = \frac{4N \times I_D}{N \times I_D + I_R} \quad (1)$$

$$y = \frac{200N \times I_R}{N \times I_D + I_R} \quad (2)$$

where I_D is the desk current and I_R is the ring current. N is the current collection efficiency (0.37) of RRDE.

The electron transfer number (n) was also calculated from the Koutecky-Levich (K-L)

equation:

$$\frac{1}{J} = \frac{1}{J_L} + \frac{1}{J_K} = \frac{1}{B\omega^{\frac{1}{2}}} + \frac{1}{J_K} \quad (3)$$

$$B = 0.62\mathrm{nF}C_0 D_0^{\frac{2}{3}} V^{-\frac{1}{6}} \quad (4)$$

where J is the measured current density, J_L is the limiting current densities and J_K is the kinetic-limiting current density, ω is the angular velocity of the disk, n is the electron transfer number, F is the Faraday constant (96485 C mol^{-1}), C_0 is the bulk concentration of O_2 (1.2×10^{-6} mol cm^{-3}), D_0 is the diffusion coefficient of O_2 (1.9×10^{-5} cm^2 s^{-1}), and V is the kinematic viscosity of the electrolyte (0.01 cm^2 s^{-1}).

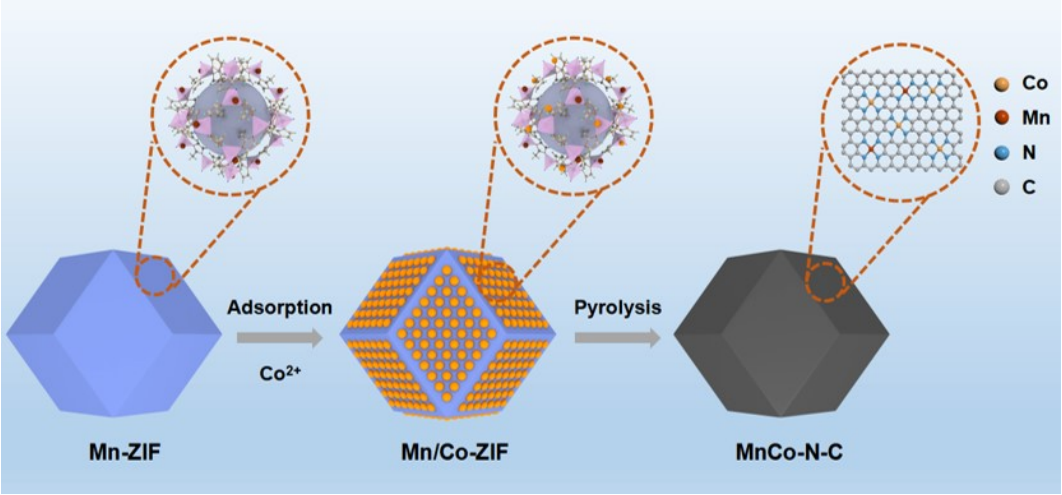

Fig. S1. Schematic of the preparation procedure of the MnCo-N-C catalyst.

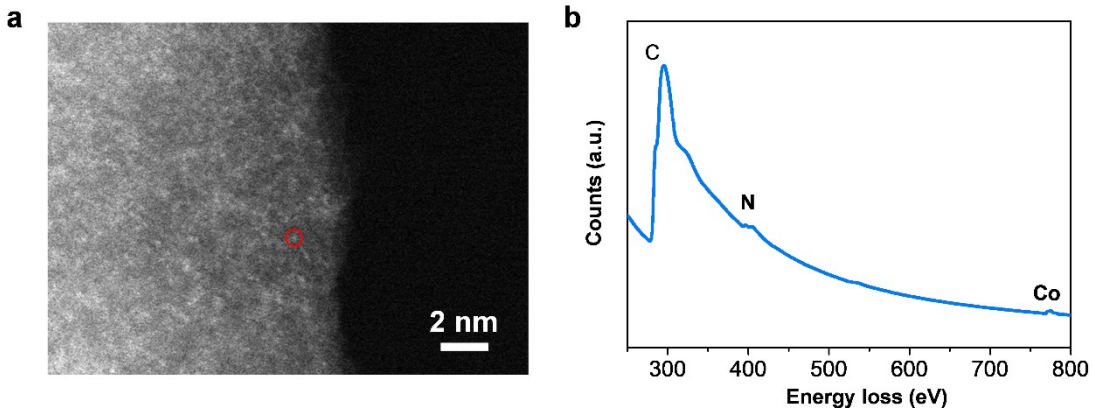

Fig. S2. (a) HAADF-STEM image of MnCo-N-C sample and (b) EEL point spectrum.

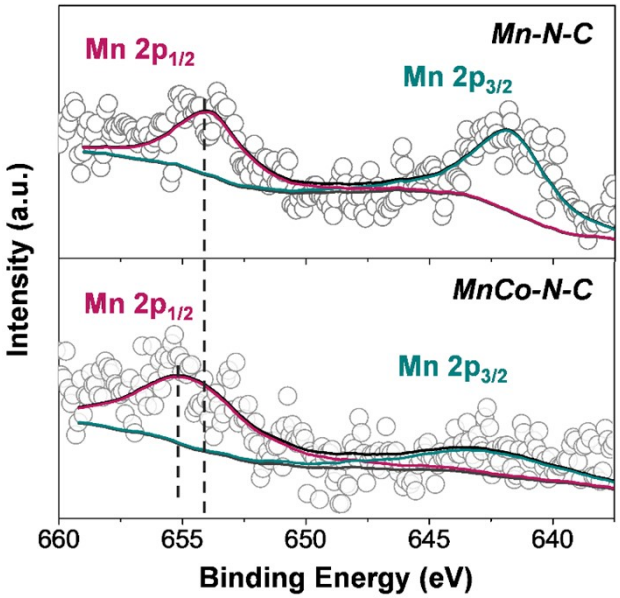

Fig. S3. High-resolution Mn 2p XPS spectra of Mn-N-C and MnCo-N-C samples.

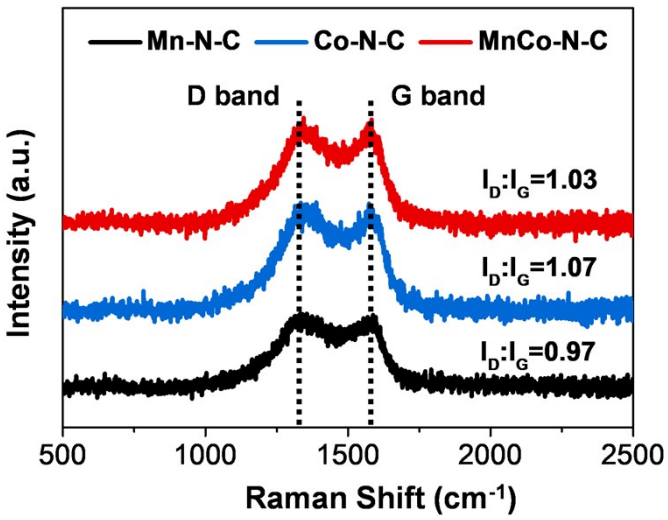

Fig. S4. Raman spectra of Mn-N-C, Co-N-C and MnCo-N-C samples.

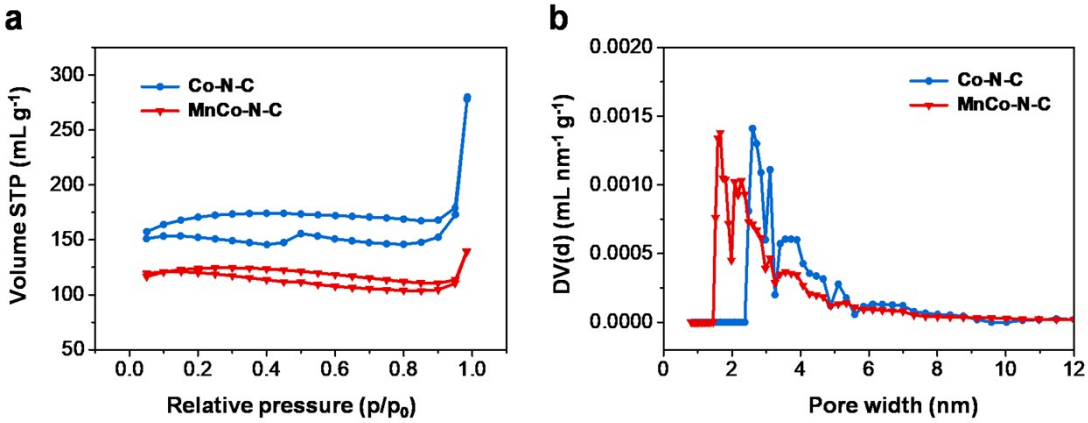

Fig. S5. (a) N_2 adsorption-desorption isotherms and (b) pore size distribution curves of Co-N-C and MnCo-N-C samples.

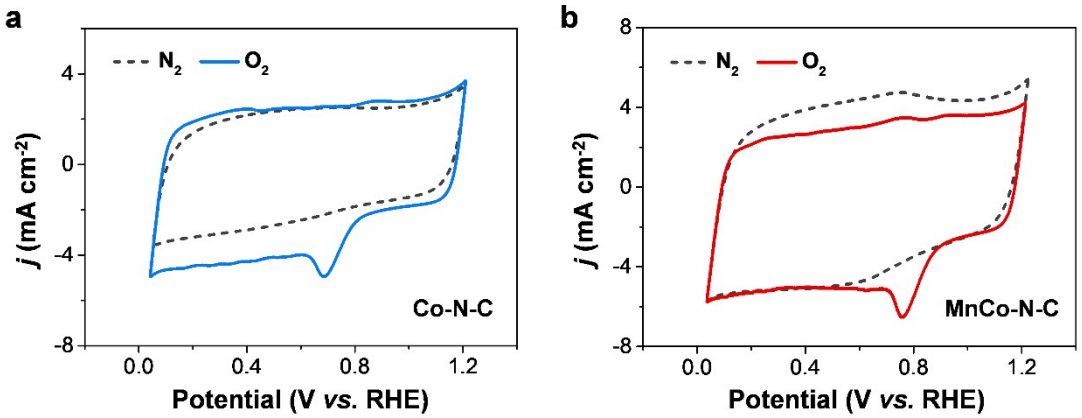

Fig. S6. (a, b) CV curves of Co-N-C and MnCo-N-C catalysts in N_2- and O_2-saturated 0.5 M H_2SO_4 aqueous electrolytes, respectively.

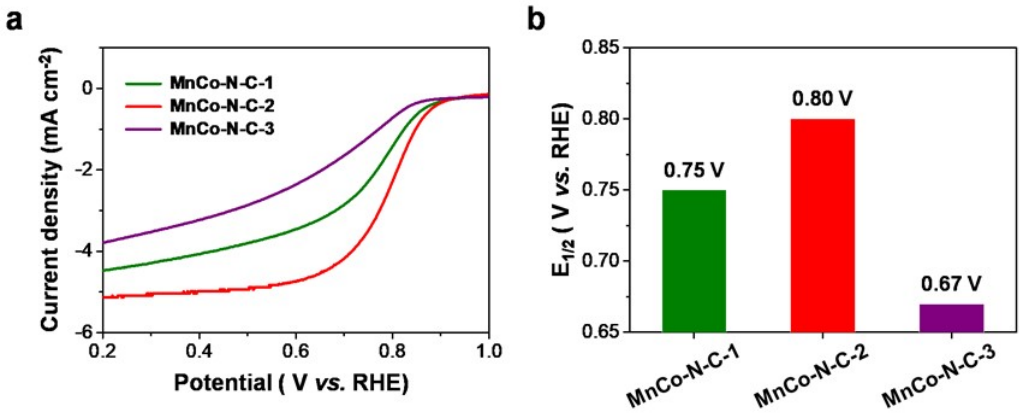

Fig. S7. LSV curves of MnCo-N-C catalysts prepared with different ratios of Mn/Co precursors.

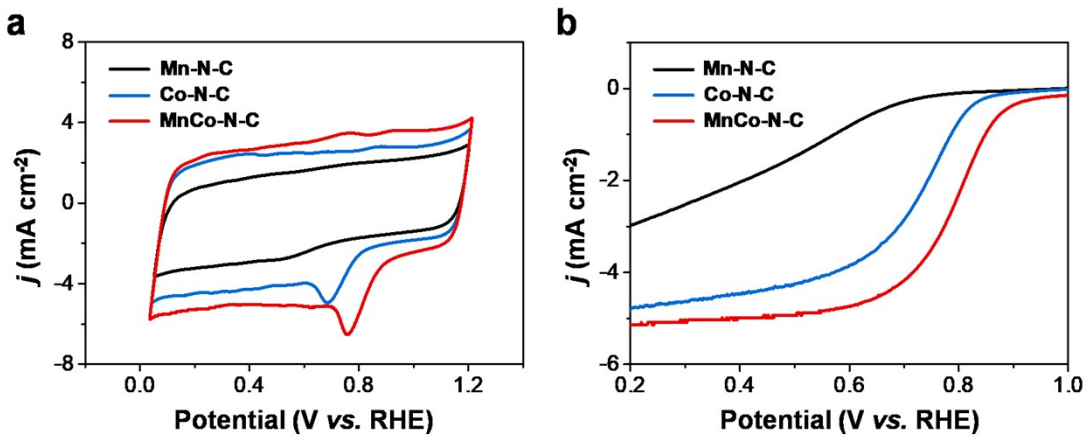

Fig. S8. (a) CV curves and (b) LSV curves of Mn-N-C, Co-N-C and MnCo-N-C catalysts.

As shown in the CV curves (Fig. S8a), the reduction peak of Mn-N-C catalyst is more negative than those of Co-N-C and MnCo-N-C catalysts, which suggest its lower activity for acidic ORR. The LSV curves in Fig. S8b indicate that the half-wave potential of Mn-N-C (0.50 V vs. RHE) is lower than those of Co-N-C (0.70 V vs. RHE) and MnCo-N-C (0.80 V vs. RHE), indicating the poor activity of Mn-N-C towards acidic ORR

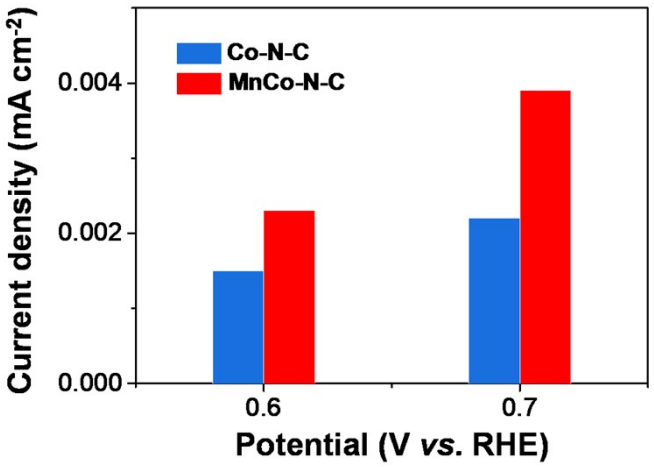

Fig. S9. Comparison of specific activities of Co-N-C and MnCo-N-C catalysts by normalizing the currents to the specific surface areas from N_2 adsorption-desorption analysis.

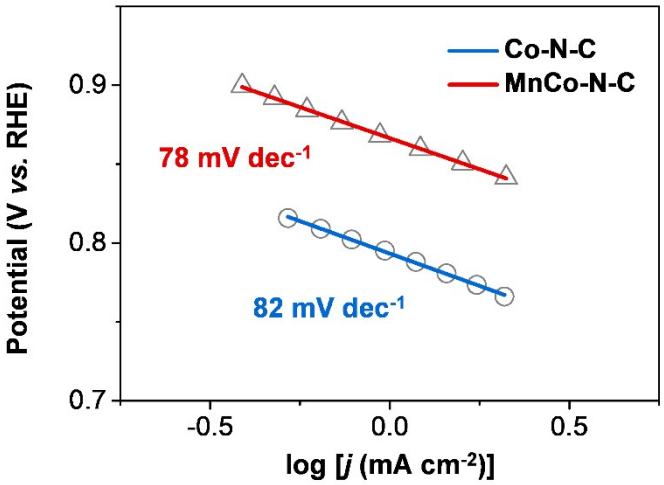

Fig. S10. Tafel plots of Co-N-C and Co/Mn-N-C catalysts.

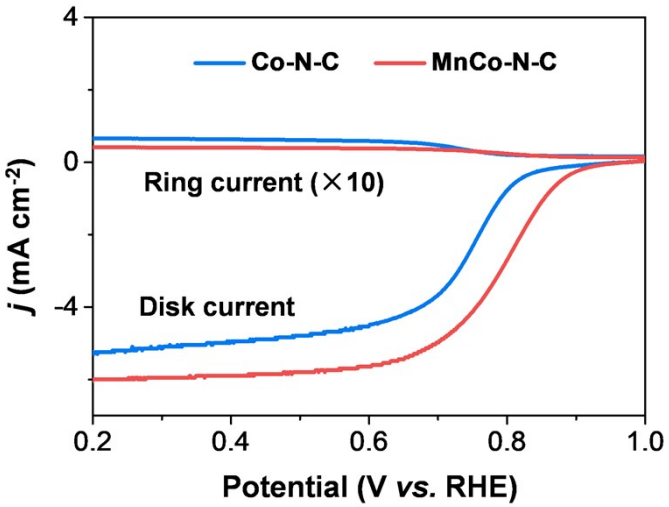

Fig. S11. LSV curves of Co-N-C and Co/Mn-N-C catalysts using RRDE method in 0.5 M H_2SO_4 aqueous solution with the rotation speed of 1600 rpm at 10 mV s^{-1}.

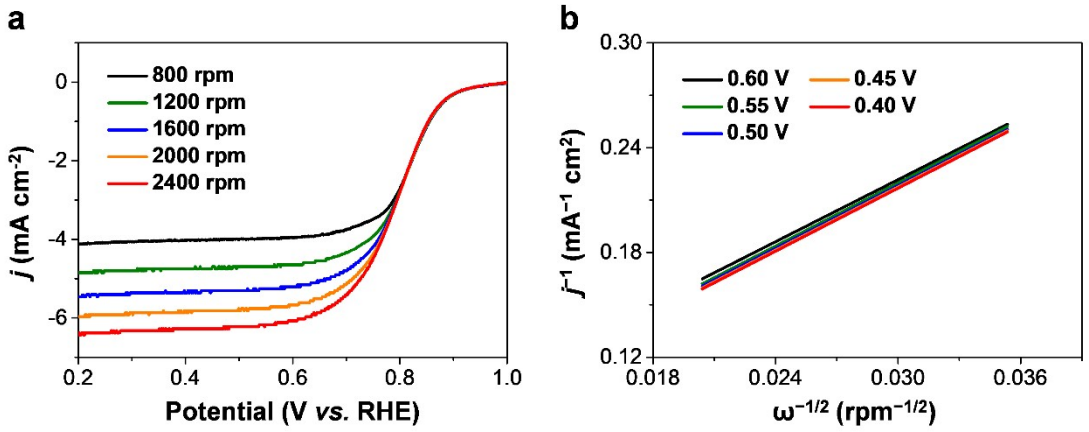

Fig. S12. (a) LSV curves of the MnCo-N-C catalyst in O_2-saturated 0.5 M H_2SO_4 aqueous solution at different rotation speed from 800 to 2400 rpm. (b) K-L plots of MnCo-N-C catalyst.

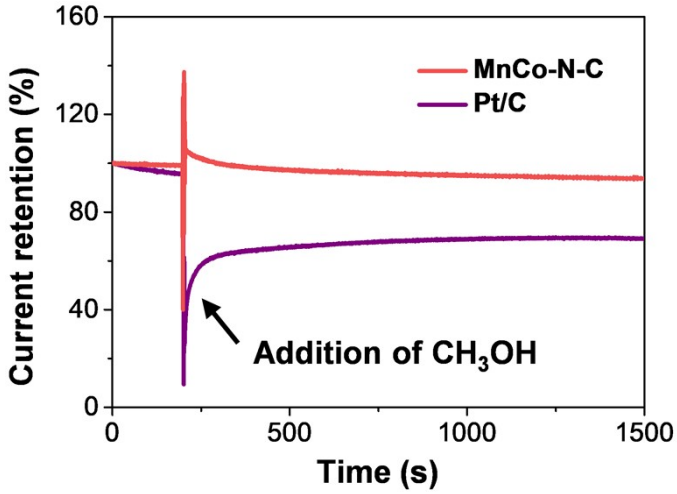

Fig. S13. The *i*-t curves of MnCo-N-C and Pt/C catalysts in O_2-saturated 0.5 M H_2SO_4 aqueous solution at a constant potential of 0.7 V (vs. RHE) before and after addition of methyl alcohol.

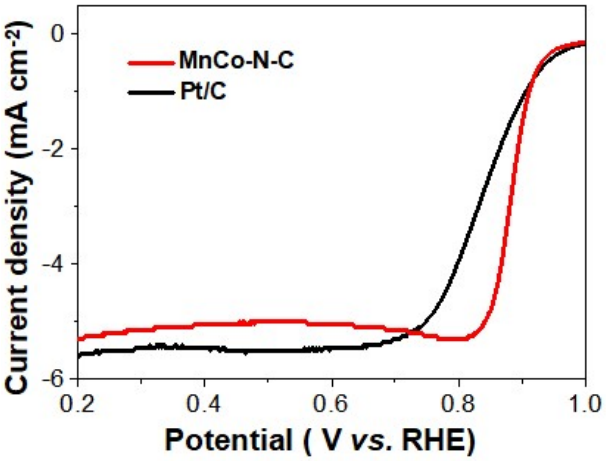

Fig. S14. LSV curves of MnCo-N-C and Pt/C catalysts in O_2-saturated 0.1 M KOH aqueous electrolytes.

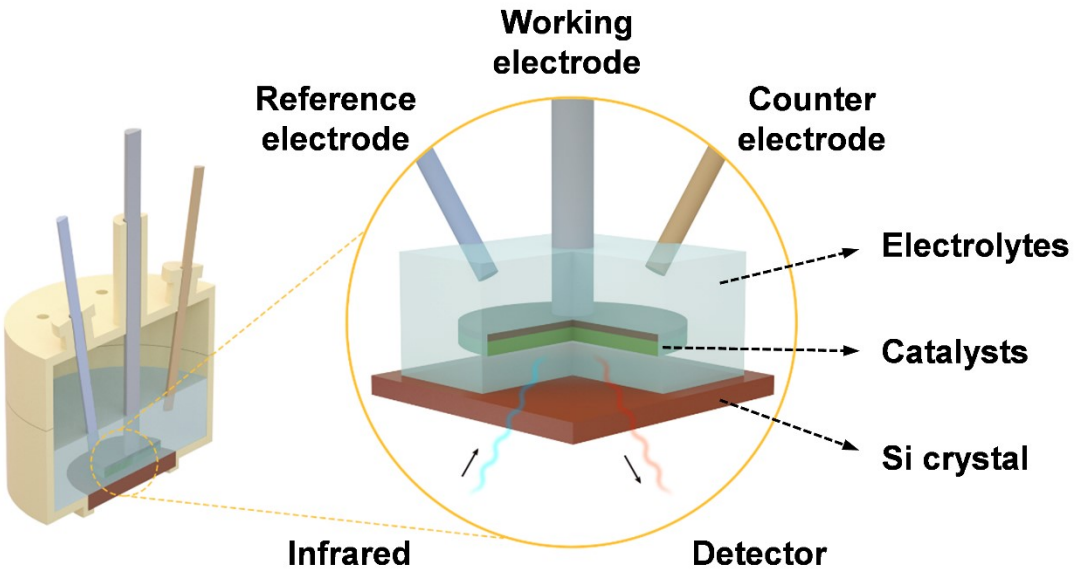

Fig. S15. Schematic of the electrochemical cell in the ATR-SEIRAS experiments.

Table S1. Content of metal elements in the Co-N-C and MnCo-N-C samples from ICP-MS analysis.

Sample	Mn (wt%)	Co (wt%)
Co-N-C	/	0.5
MnCo-N-C	0.6	1.0

Table S2. The peak fitting results of N 1s XPS data of Co-N-C and MnCo-N-C.

Catalyst	pyridinic N (%)	Metal-N (%)	pyrrolic N (%)	graphitic N (%)
Co-N-C	48.6	19.6	21.4	10.4
MnCo-N-C	32.6	32.0	16.0	19.4

References

1. J. Wang, Z. Q. Huang, W, Liu, C. Chang, H. L. Tang, Z. J. Li, W. X. Chen, C. J. Jia, T. Yao, S. Q. Wei, Y. Wu and Y. D. Li, *J. Am. Chem. Soc.*, 2017, **139**, 17281-17284.
2. H. J. Fan, M. Knez, R. Scholz, K. Nielsch, E. Pippel, D. Hesse, M. Zacharias and U. Gösele, *Nat. Mater.*, 2006, **5**, 627-631.